Selective Detection of nano-molar range Noxious Anions in Water by a Luminescent Metal-Organic Framework

Pooja Daga,[a] Sourav Sarkar,[b] Prakash Majee,[a] Debal Kanti Singha,[a,b] Sayani Hui,[b] Partha Mahata[b*] and Sudip Kumar Mondal[a*]

[a]Department of Chemistry, Siksha-Bhavana, Visva-Bharati University, Santiniketan-731235, West Bengal, India. Email: sudip.mondal@visva-bharati.ac.in

[b]Department of Chemistry, Jadavpur University, Jadavpur, Kolkata-700 032, West Bengal, India.

Email: parthachem@gmail.com

ELECTRONIC SUPPLEMENTARY INFORMATION

[*] Corresponding Authors, E-mail: sudip.mondal@visva-bharati.ac.in, parthachem@gmail.com

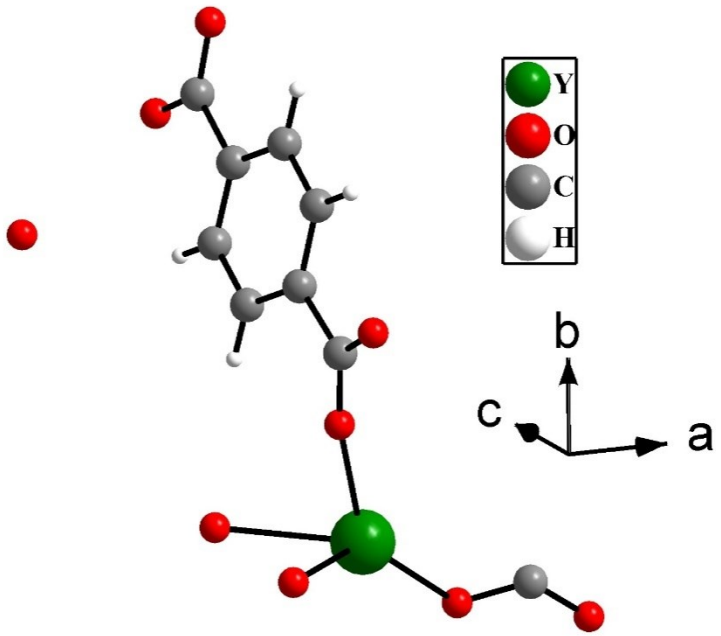

Figure S1. The figure shows the asymmetric unit of compound **1**. The hydrogen atoms of water molecules are not shown.

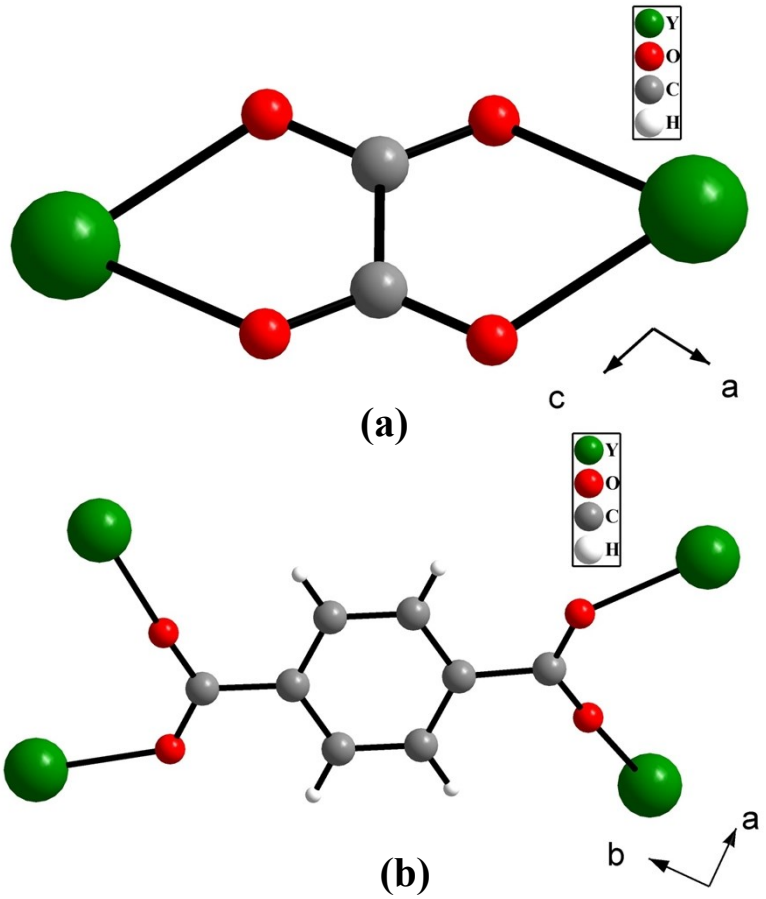

Figure S2. The figure shows the coordination modes of oxalate (a) and terephthalate ion (b) in compound **1**.

Table S1: Selected bond distances (Å) observed in $[Y(tp)(ox)_{0.5}(H_2O)_2]\cdot H_2O$ (tp = terephthalate, ox = oxalate), **1**.

Bond	Distances, Å	Bond	Distances, Å
Y(1)-O(1)	2.256(4)	Y(1)-O(5)	2.398(4)
Y(1)-O(3)#1	2.271(4)	Y(1)-O(6)#4	2.442(4)
Y(1)-O(4)#2	2.316(4)	Y(1)-O(8)	2.451(5)
Y(1)-O(2)#3	2.331(4)	Y(1)-O(7)	2.460(4)

Symmetry transformations used to generate equivalent atoms: #1 x,-y+3/2,z-1/2 #2 -x+1,y-1/2,-z+1/2 #3 -x+2,-y+1,-z+1 #4 -x+2,-y+1,-z

Table S2: Selected bond angles observed in $[Y(tp)(ox)_{0.5}(H_2O)_2]\cdot H_2O$ (tp = terephthalate, ox = oxalate), **1**.

Angle	Amplitude (º)	Angle	Amplitude (º)
O(1)-Y(1)-O(3)#1	89.97(15)	O(4)#2-Y(1)-O(5)	74.66(15)
O(1)-Y(1)-O(4)#2	144.13(16)	O(2)#3-Y(1)-O(5)	75.53(15)
O(3)#1-Y(1)-O(4)#2	103.90(15)	O(1)-Y(1)-O(6)#4	75.70(15)
O(1)-Y(1)-O(2)#3	103.59(15)	O(3)#1-Y(1)-O(6)#4	82.54(15)
O(3)#1-Y(1)-O(2)#3	147.46(16)	O(4)#2-Y(1)-O(6)#4	138.13(14)
O(4)#2-Y(1)-O(2)#3	82.30(15)	O(2)#3-Y(1)-O(6)#4	72.71(15)
O(1)-Y(1)-O(5)	141.20(15)	O(5)-Y(1)-O(6)#4	66.96(13)
O(3)#1-Y(1)-O(5)	75.51(16)	O(1)-Y(1)-O(8)	78.36(16)
O(3)#1-Y(1)-O(8)	72.37(16)	O(3)#1-Y(1)-O(7)	140.99(17)
O(4)#2-Y(1)-O(8)	74.82(16)	O(4)#2-Y(1)-O(7)	73.97(15)
O(2)#3-Y(1)-O(8)	138.89(16)	O(2)#3-Y(1)-O(7)	71.54(16)
O(5)-Y(1)-O(8)	128.05(14)	O(5)-Y(1)-O(7)	136.83(14)
O(6)#4-Y(1)-O(8)	143.64(14)	O(6)#4-Y(1)-O(7)	125.67(14)
O(1)-Y(1)-O(7)	74.60(16)	O(8)-Y(1)-O(7)	69.53(16)

Symmetry transformations used to generate equivalent atoms: #1 x,-y+3/2,z-1/2 #2 -x+1,y-1/2,-z+1/2 #3 -x+2,-y+1,-z+1 #4 -x+2,-y+1,-z

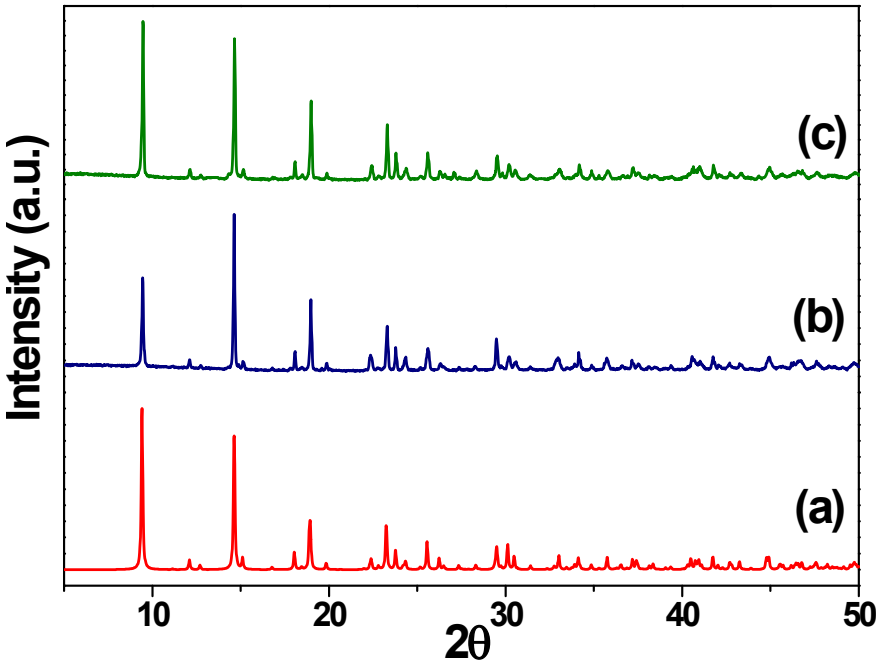

Figure S3. Powder XRD (CuKα) patterns of (a) **1** (simulated from single crystal X-ray data), (b) **1** (experimental) and (c) **1a (**experimental).

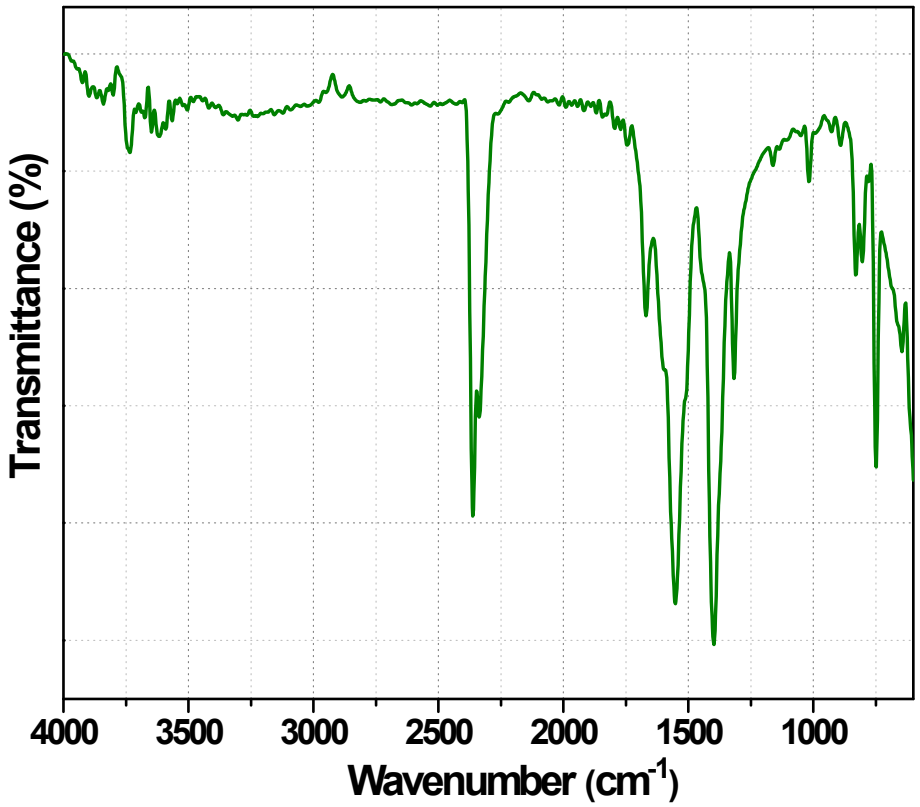

Figure S4. FTIR spectrum of **1**.

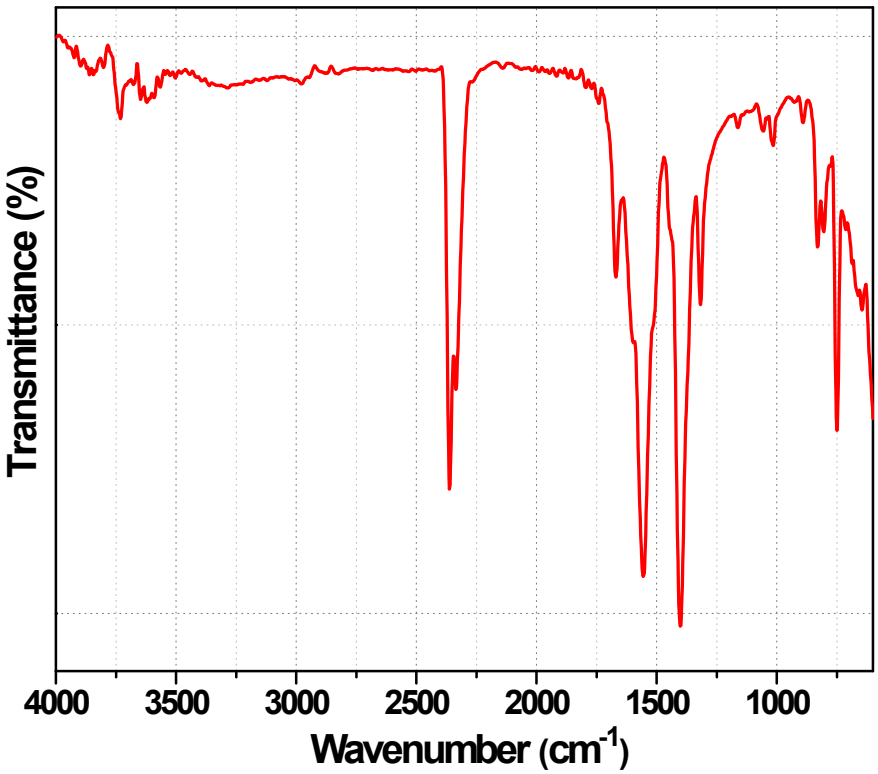

Figure S5. FTIR spectrum of **1a**.

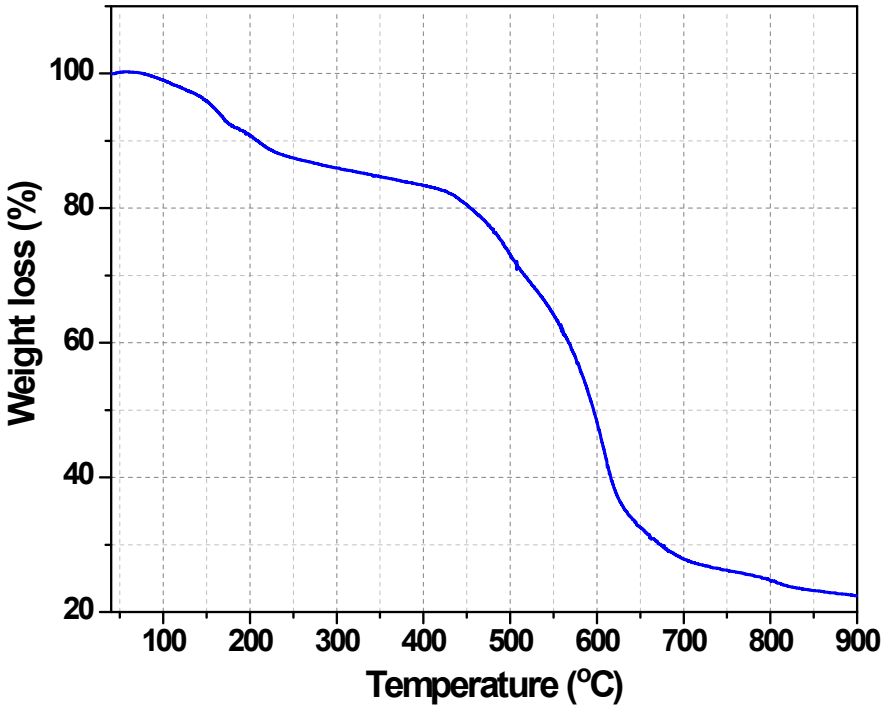

Figure S6. Thermogravimetric analysis (TGA) data of **1**, in a nitrogen atmosphere. The plot shows % weight loss of **1** with the increase in temperature.

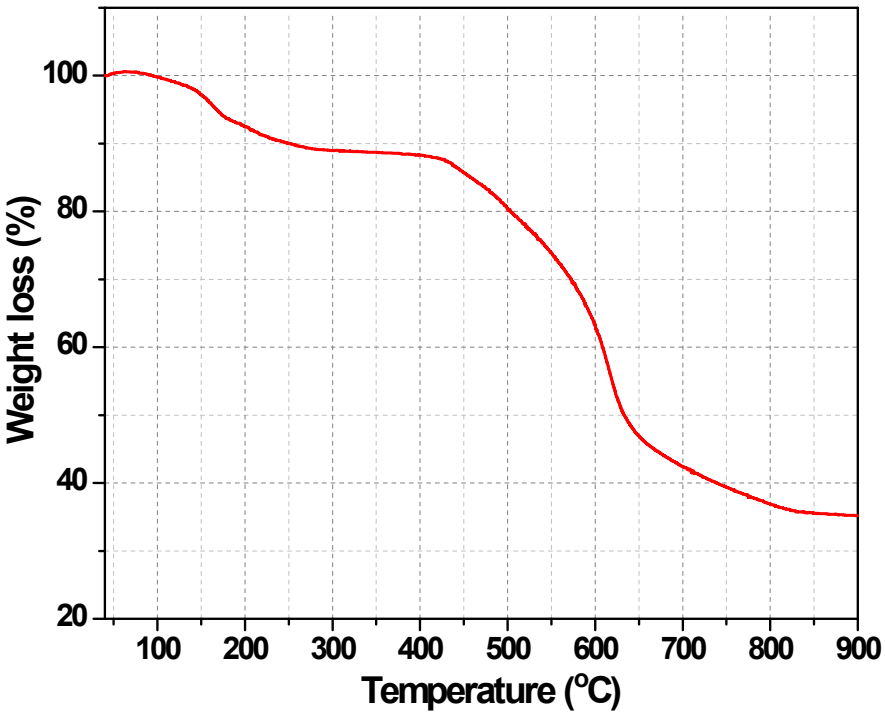

Figure S7. Thermogravimetric analysis (TGA) data of **1a**, in a nitrogen atmosphere. The plot shows % weight loss of **1a** with the increase in temperature.

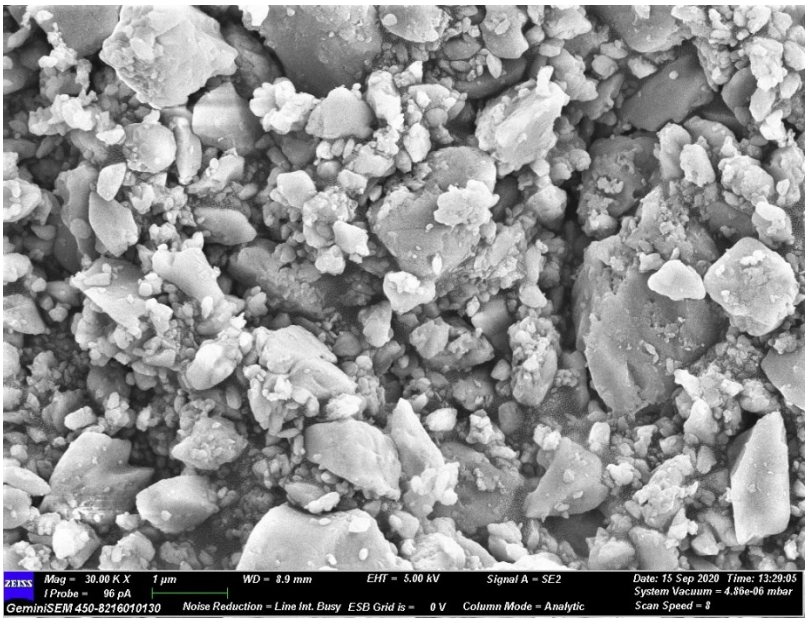

Figure S8. SEM image of **1a**.

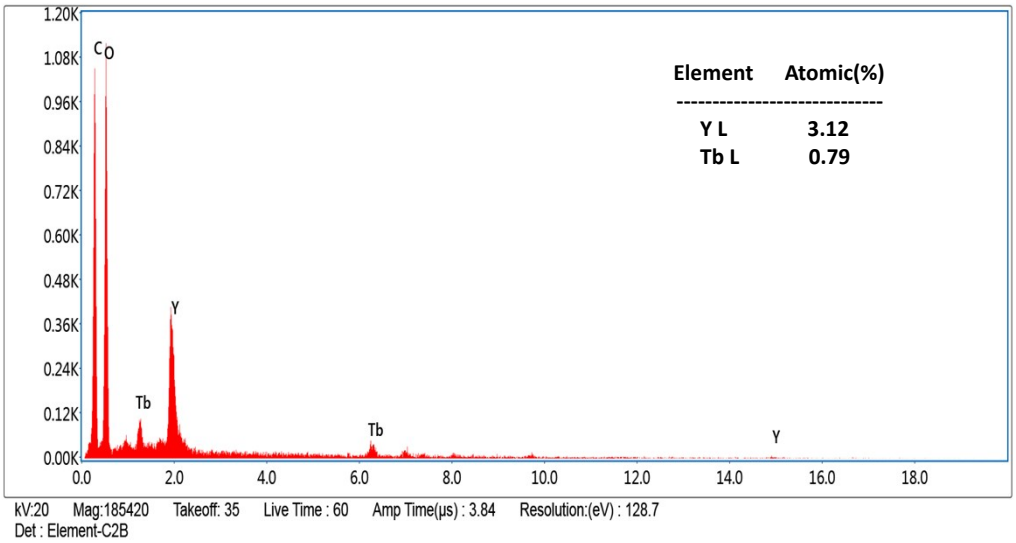

Figure S9. Representative EDX plot of **1a.** The figure demonstrates that Tb and Y are present in the molar ratio of ~ 1:4.

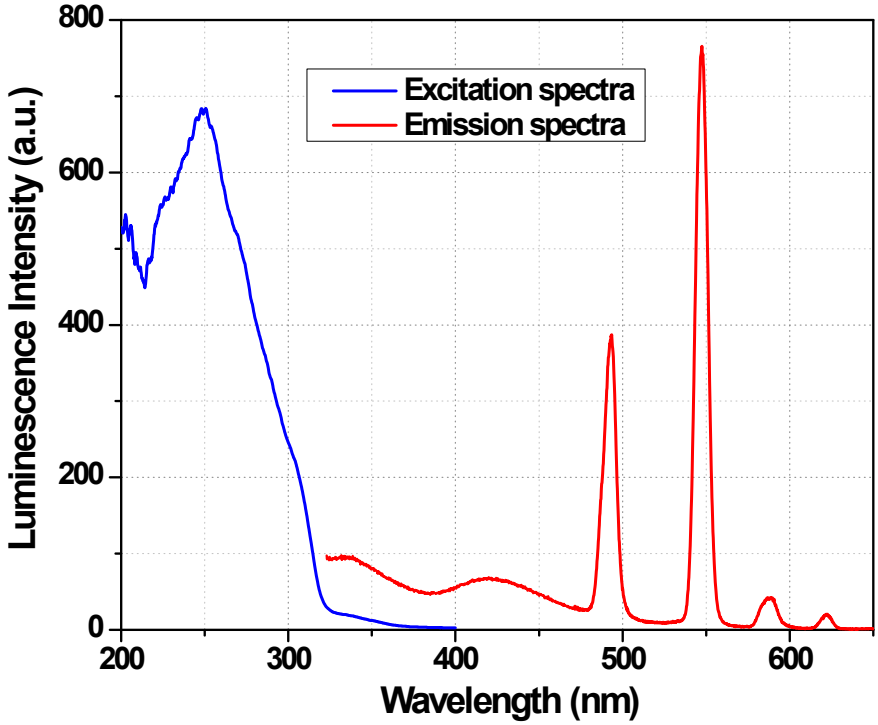

Figure S10. Excitation and emission spectra of **1a.** Emission spectra of both ligand-centered and metal-centered were shown here. The excitation wavelength was chosen at 280 nm for emission spectra and for the excitation spectra, emission was fixed at 546 nm.

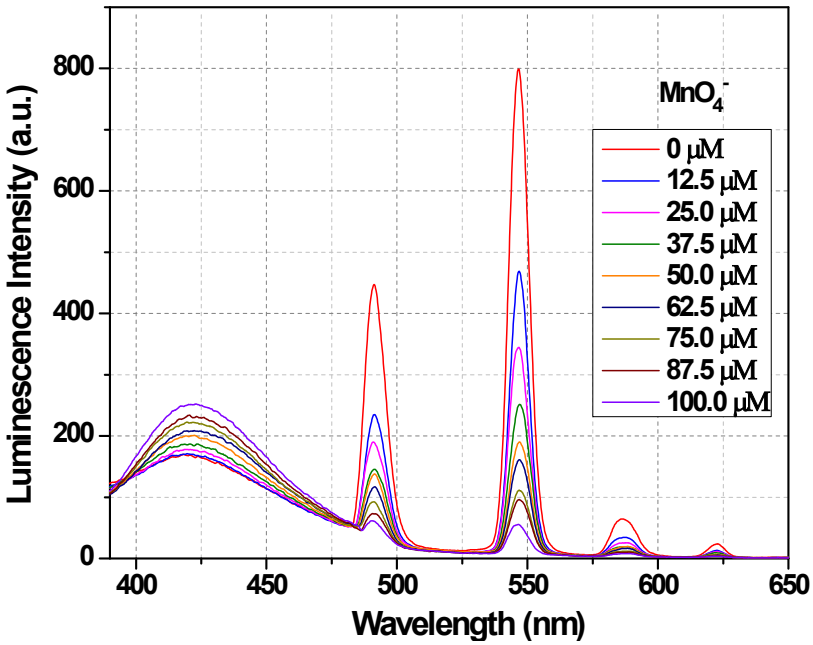

Figure S11. Luminescence spectra of **1a** dispersed in aqueous solution upon the incremental addition of an aqueous solution of MnO_4^- ions (λ_{ex} = 280 nm). The final concentration of MnO_4^- ions in the medium is indicated in the legend.

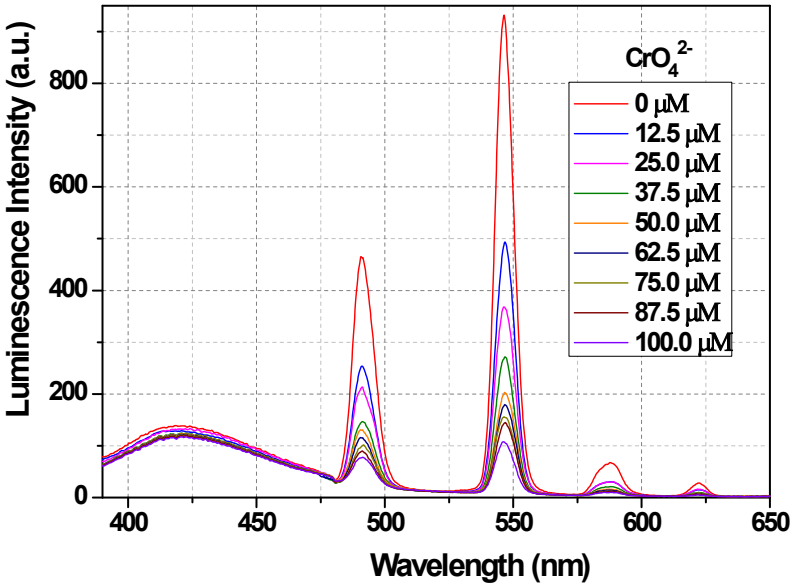

Figure S12. Luminescence spectra of **1a** dispersed in aqueous solution upon the incremental addition of an aqueous solution of CrO_4^{2-} ions (λ_{ex} = 280 nm). The final concentration of CrO_4^{2-} ions in the medium is indicated in the legend.

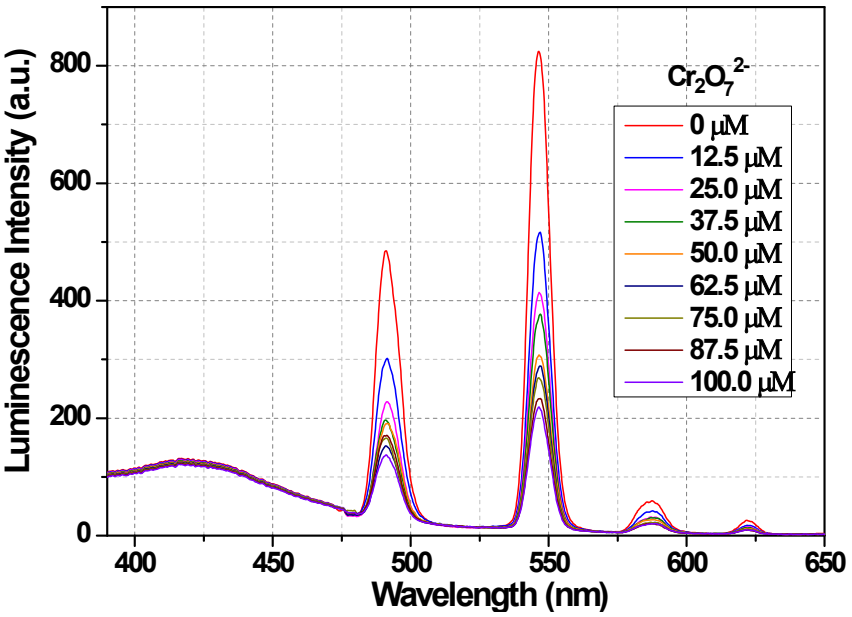

Figure S13. Luminescence spectra of **1a** dispersed in aqueous solution upon the incremental addition of an aqueous solution of $Cr_2O_7^{2-}$ ions (λ_{ex} = 280 nm). The final concentration of $Cr_2O_7^{2-}$ ions in the medium is indicated in the legend.

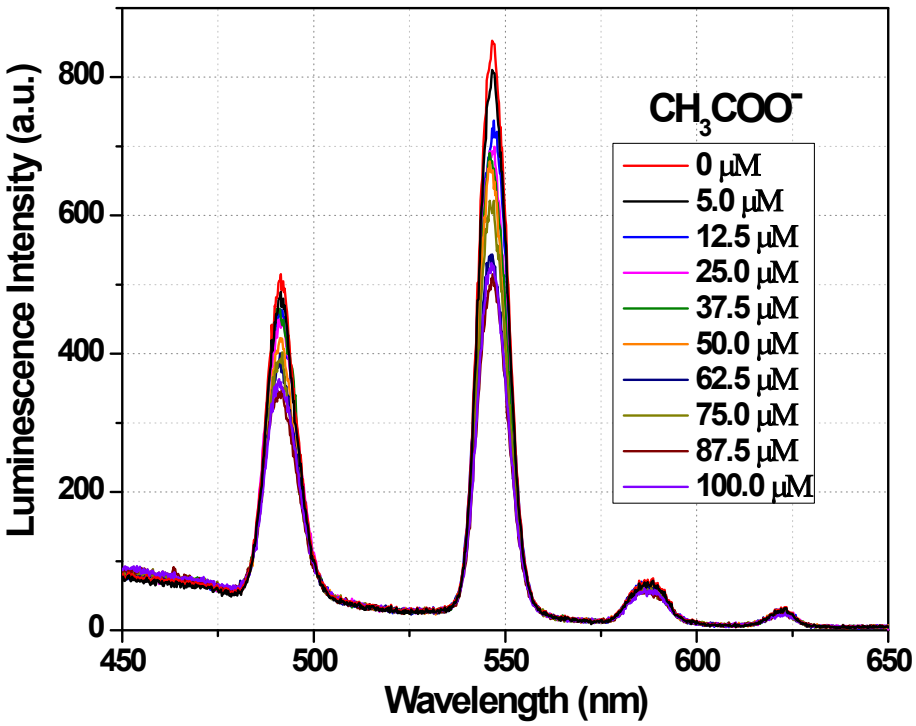

Figure S14: Luminescence spectra of **1a** dispersed in aqueous solution upon the incremental addition of an aqueous solution of CH_3COO^- ions (λ_{ex} = 280 nm). The final concentration of CH_3COO^- ions in the medium is indicated in the legend.

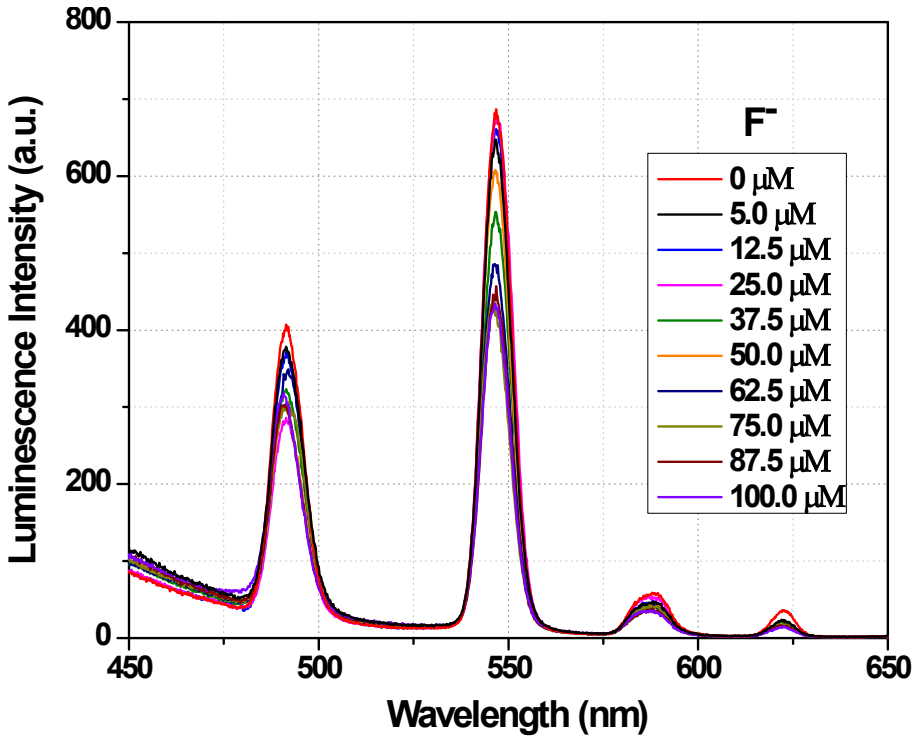

Figure S15. Luminescence spectra of **1a** dispersed in aqueous solution upon the incremental addition of an aqueous solution of F^- ions (λ_{ex} = 280 nm). The final concentration of F^- ions in the medium is indicated in the legend.

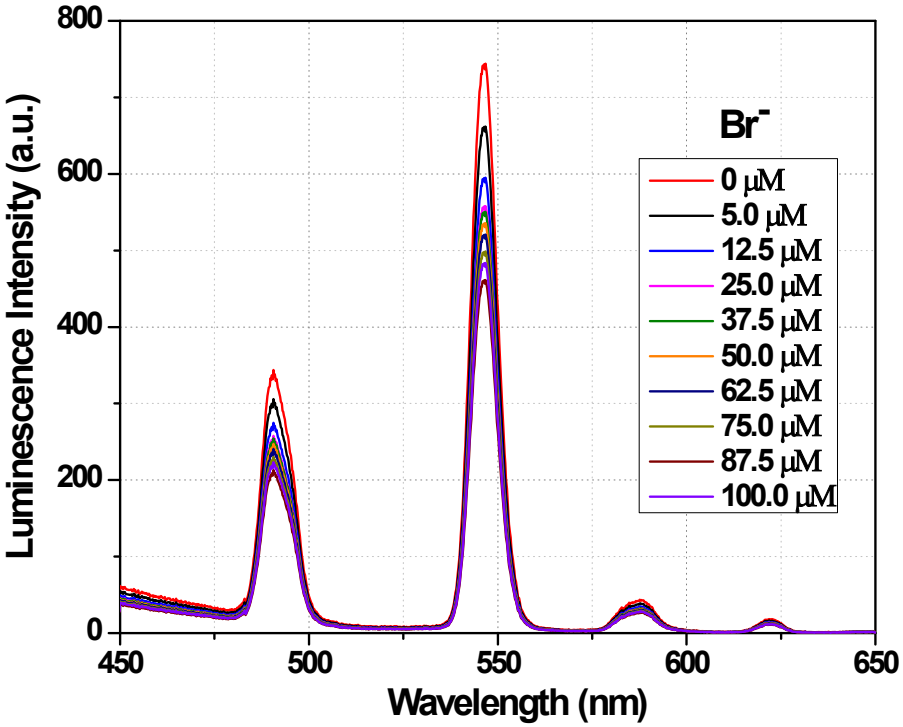

Figure S16. Luminescence spectra of **1a** dispersed in aqueous solution upon the incremental addition of an aqueous solution of Br^- ions (λ_{ex} = 280 nm). The final concentration of Br^- ions in the medium is indicated in the legend.

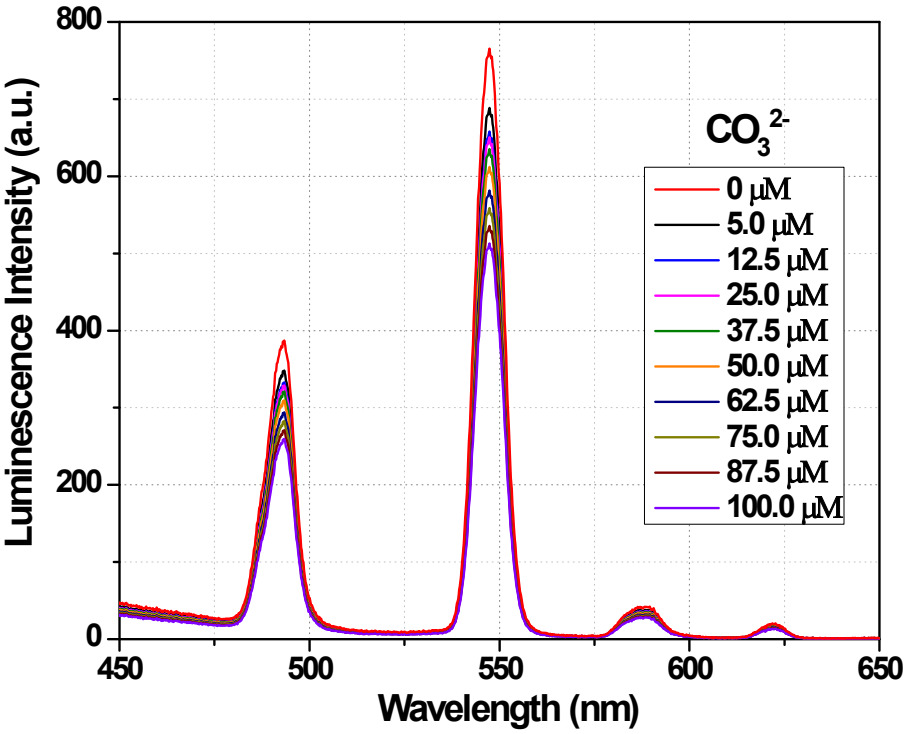

Figure S17. Luminescence spectra of **1a** dispersed in aqueous solution upon the incremental addition of an aqueous solution of CO_3^{2-} ions (λ_{ex} = 280 nm). The final concentration of CO_3^{2-} ions in the medium is indicated in the legend.

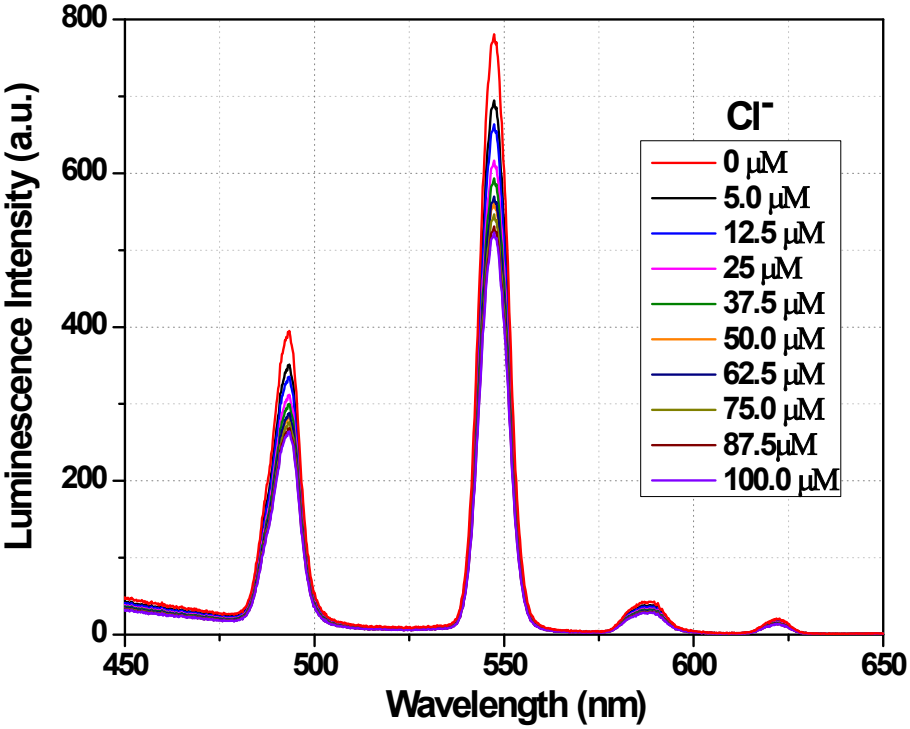

Figure S18. Luminescence spectra of **1a** dispersed in aqueous solution upon the incremental addition of an aqueous solution of Cl^- ions (λ_{ex} = 280 nm). The final concentration of Cl^- ions in the medium is indicated in the legend.

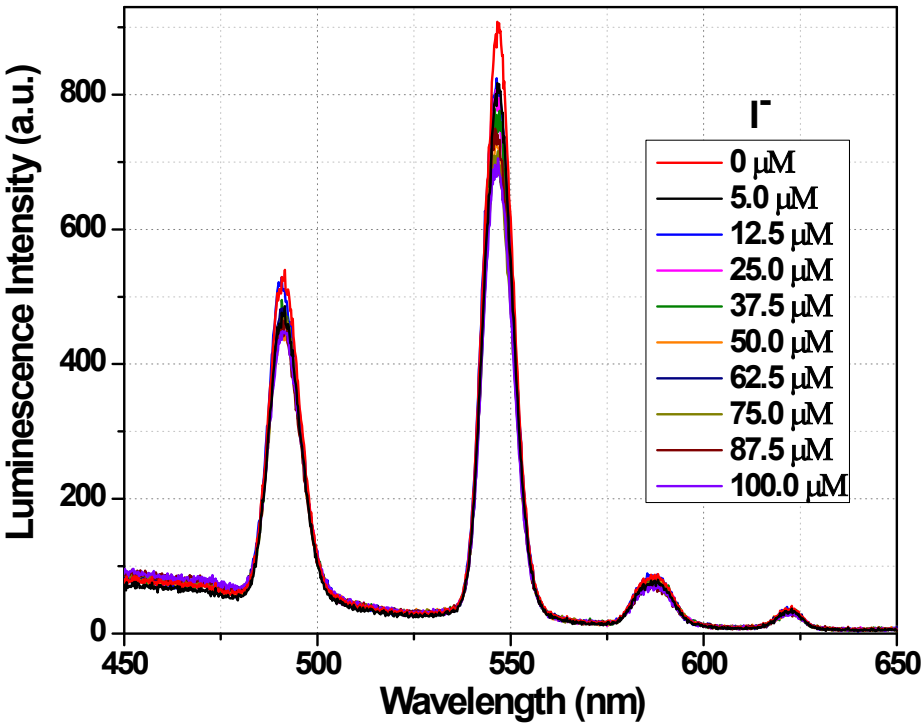

Figure S19. Luminescence spectra of **1a** dispersed in aqueous solution upon the incremental addition of an aqueous solution of I^- ions (λ_{ex} = 280 nm). The final concentration of I^- ions in the medium is indicated in the legend.

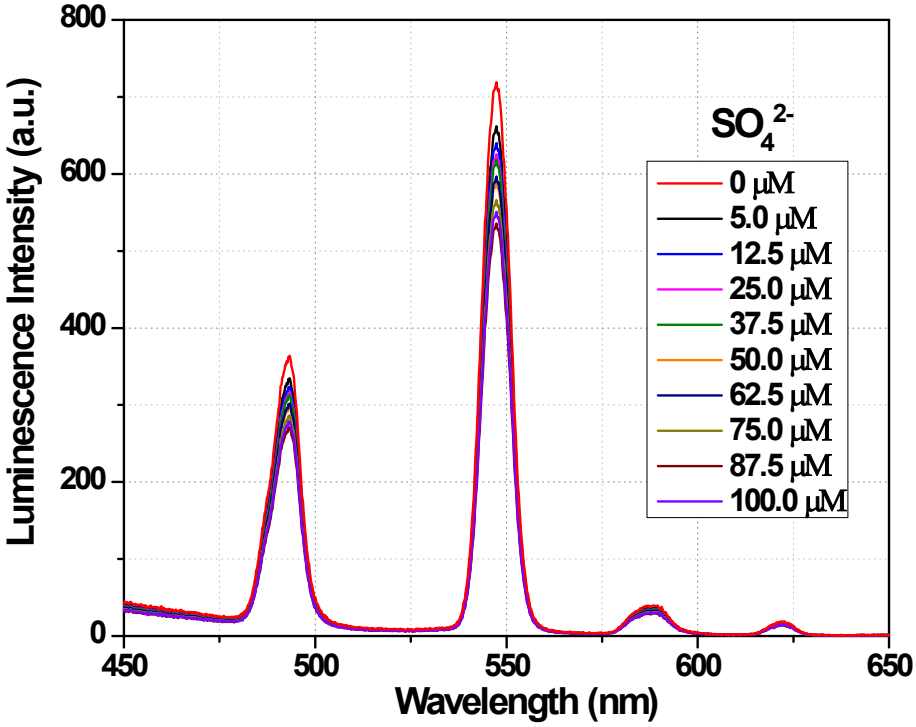

Figure S20. Luminescence spectra of **1a** dispersed in aqueous solution upon the incremental addition of an aqueous solution of SO_4^{2-} ions (λ_{ex} = 280 nm). The final concentration of SO_4^{2-} ions in the medium is indicated in the legend.

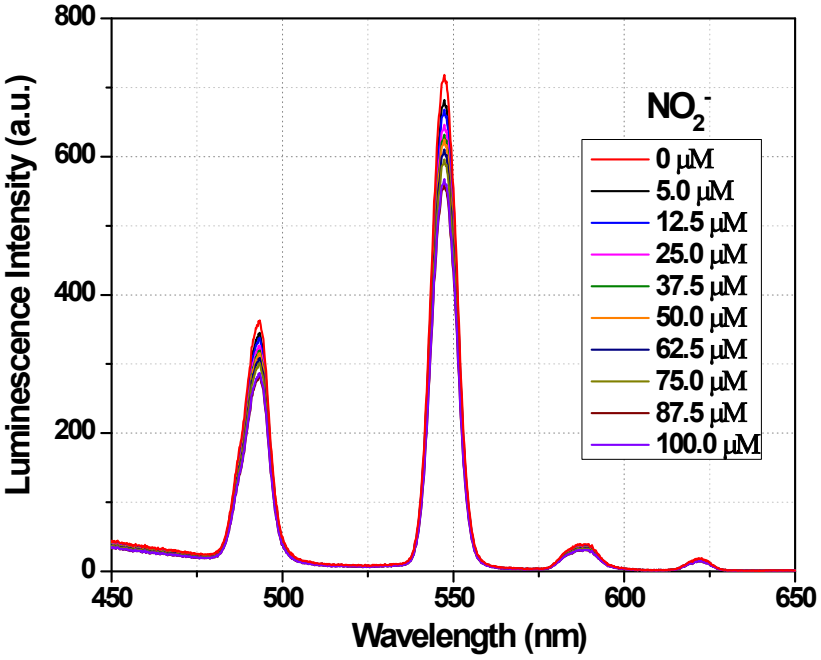

Figure S21. Luminescence spectra of **1a** dispersed in aqueous solution upon the incremental addition of an aqueous solution of NO_2^- ions (λ_{ex} = 280 nm). The final concentration of NO_2^- ions in the medium is indicated in the legend.

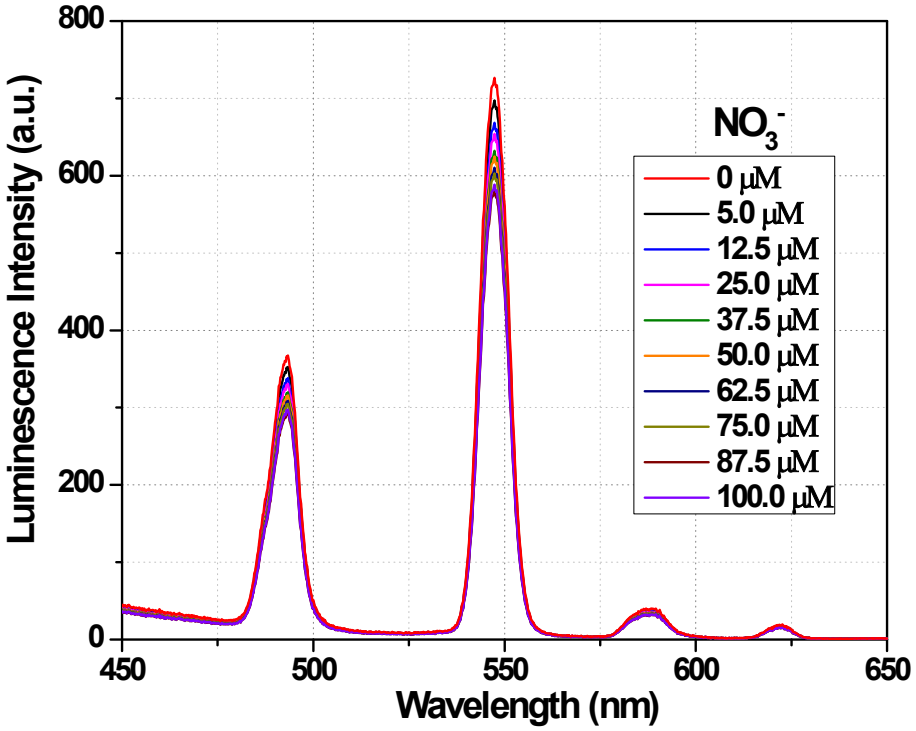

Figure S22. Luminescence spectra of **1a** dispersed in aqueous solution upon the incremental addition of an aqueous solution of NO_3^- ions (λ_{ex} = 280 nm). The final concentration of NO_3^- ions in the medium is indicated in the legend.

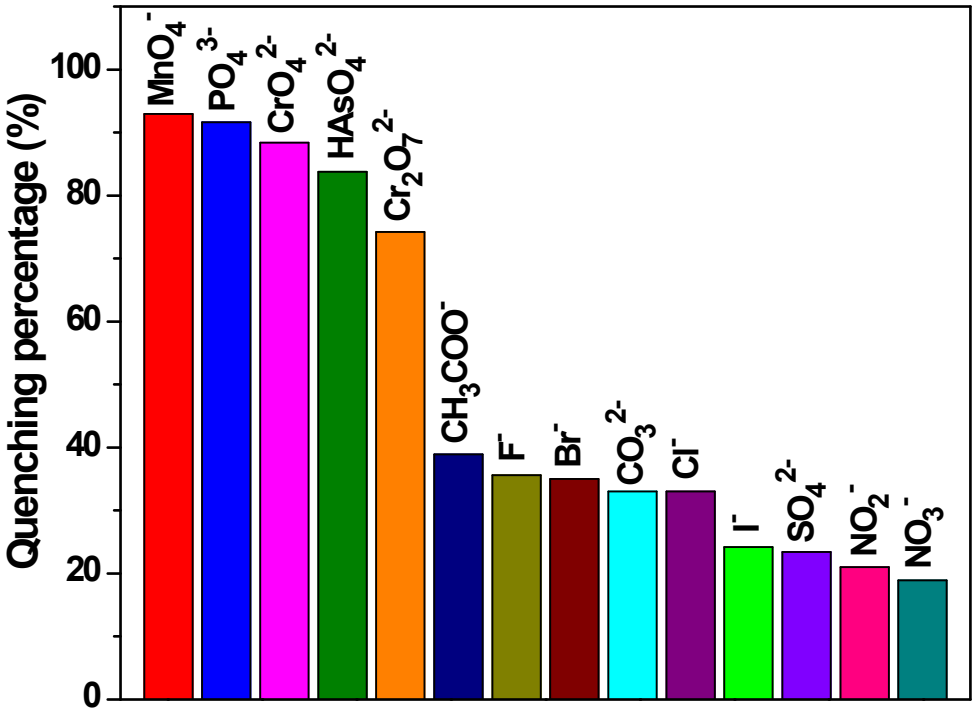

Figure S23. Quenching efficiency of **1a** toward different anions after the addition of 100μM of these anions.

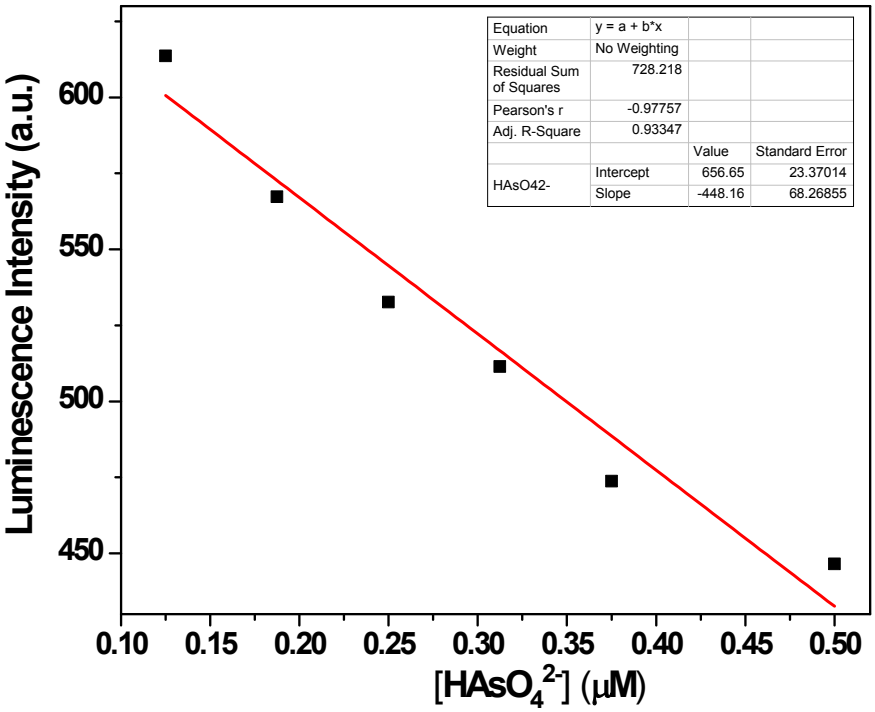

Figure S24. Linear correlation between the luminescence intensity and concentration of arsenate anion ($HAsO_4^{2-}$).

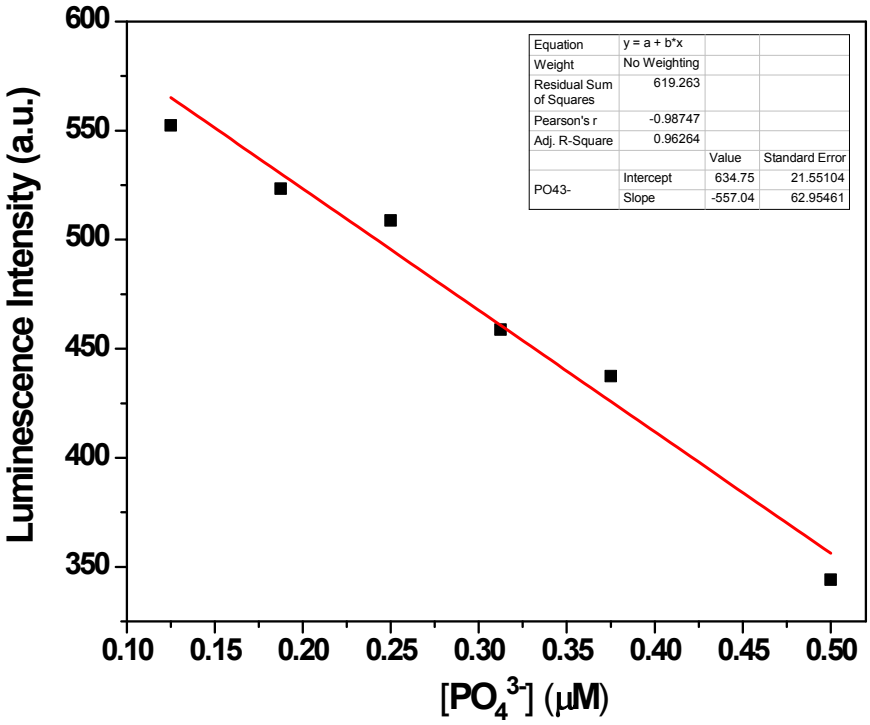

Figure S25. Linear correlation between the luminescence intensity and concentration of phosphate anion (PO_4^{3-}).

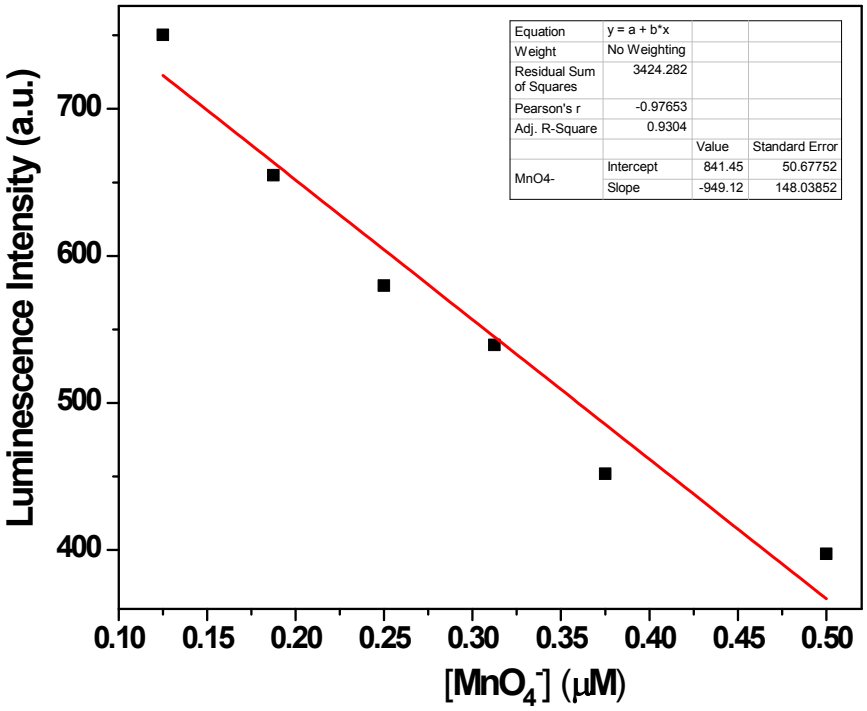

Figure S26. Linear correlation between the luminescence intensity and concentration of manganate anion (MnO_4^-).

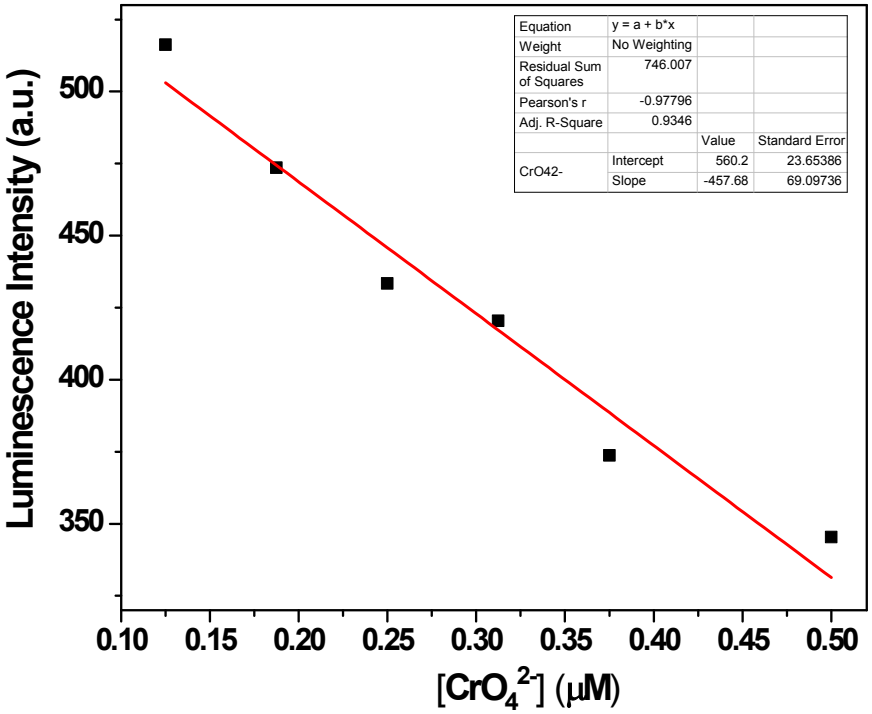

Figure S27. Linear correlation between the luminescence intensity and concentration of chromate anion (CrO_4^{2-}).

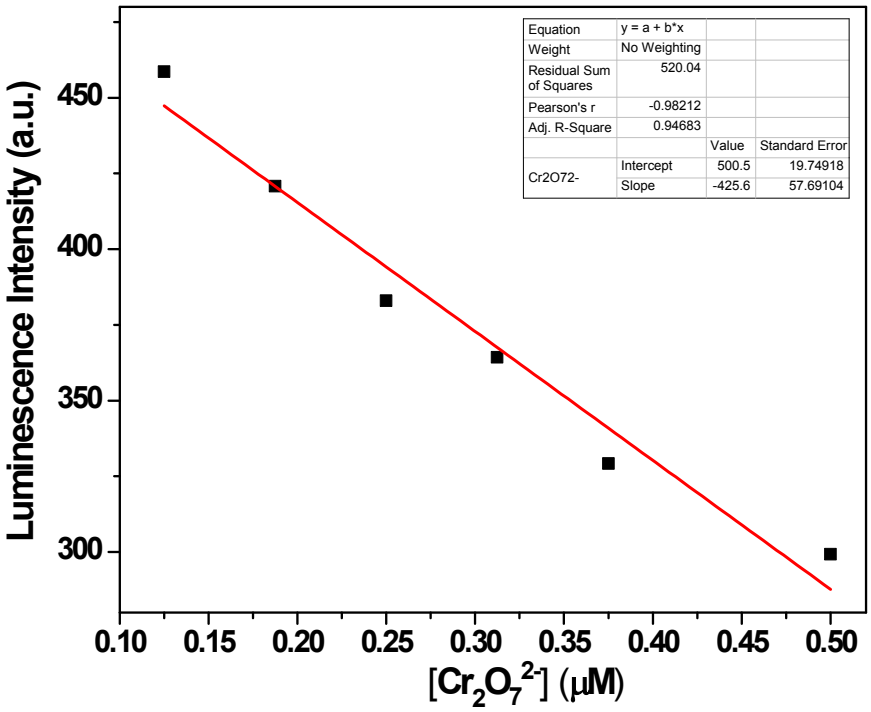

Figure S28. Linear correlation between the luminescence intensity and concentration of dichromate anion ($Cr_2O_7^{2-}$).

The limit of detection (LOD) was calculated by the following equation, LOD = 3σ/m, where σ denotes the standard deviation of the luminescence intensity (at 546 nm) of **1a** without any analytes and m represents the slope of the plot of luminescence intensity data *vs* concentration of anions.

Table S3: Calculation of standard deviation and Limit of Detection (LOD) for $HAsO_4^{2-}$, PO_4^{3-}, MnO_4^{-}, CrO_4^{2-} and $Cr_2O_7^{2-}$:

Blank Reading (only **1a**)	Luminescence intensity at 546 nm (X)	Mean (x)	Standard Deviation $(\sigma) = \sqrt{\frac{\sum \lvert X - x \rvert^2}{N}}$
Reading 1	791.7	793.2	6.23
Reading 2	782.6		
Reading 3	808.1		
Reading 4	795.2		
Reading 5	788.4		

Slope, m for $HAsO_4^{2-}$ = 448.16

Slope, m for PO_4^{3-}= 557.04

Slope, m for MnO_4^{-}= 949.12

Slope, m for CrO_4^{2-}= 457.68

Slope, m for $Cr_2O_7^{2-}$= 425.6

LOD for $HAsO_4^{2-}$ = $3\sigma/m$ = (3 × 6.23)/448.16 = 41.7 nM

LOD for PO_4^{3-} = $3\sigma/m$ = (3 × 6.23)/557.04 = 33.5 nM

LOD for MnO_4^{-} = $3\sigma/m$ = (3 × 6.23)/949.12 = 19.6 nM

LOD for CrO_4^{2-} = $3\sigma/m$ = (3 × 6.23)/457.68 = 40.8 nM

LOD for $Cr_2O_7^{2-}$ = $3\sigma/m$ = (3 × 6.23)/425.6 = 43.9 nM

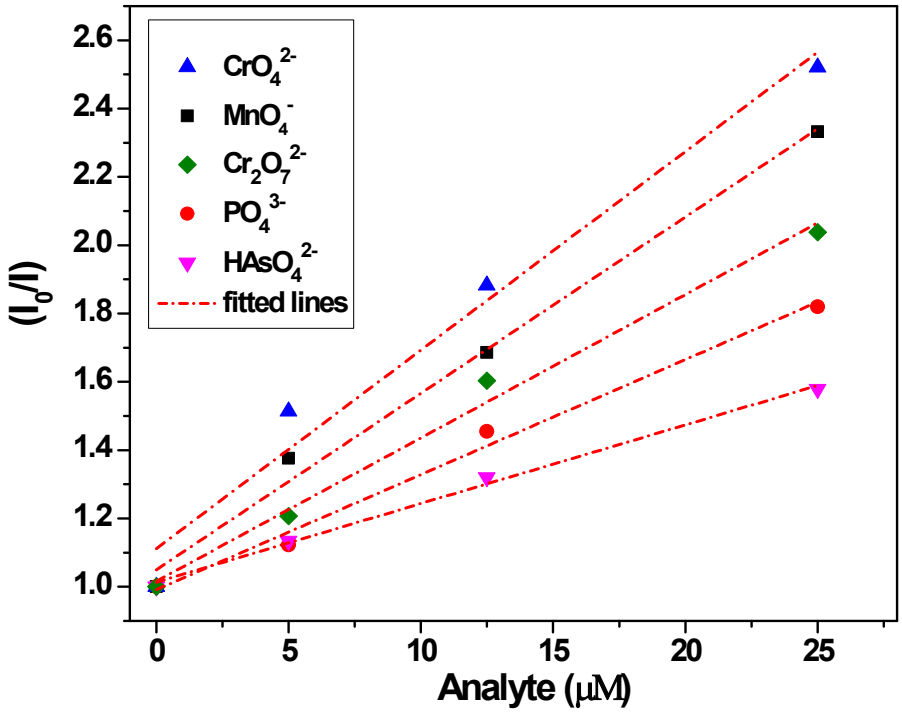

Figure S29. K_{sv} curves of **1a** in an aqueous solution in the presence of $HAsO_4^{2-}$, PO_4^{3-}, MnO_4^-, CrO_4^{2-} and $Cr_2O_7^{2-}$ anions.

Table S4: Comparison of the luminescence-based sensors for the detection of MnO_4^- anion

Sl. No.	Luminescent Sensor	Anions Detected	Medium	LOD	K_{sv}	Reference
1.	$[Mn_4(C_{20}H_{10}N_2O_4S)_2(HCOO)_4(DEF)_2]$	MnO_4^-	H_2O	69 ppb	NM	[1]
2.	$[Pb(C_{20}H_{10}N_2O_4S)(DMF)]$	MnO_4^-	H_2O	398 ppb	NM	[1]
3.	$[Cd(L)_2(H_2O)_2]_n$	MnO_4^-	H_2O	173 μM	$2.2 \times 10^4\ M^{-1}$	[2]
4.	$\{[Ba_3La_{0.5}(\mu^3\text{-}L)_{2.5}(H_2O)_3(DMF)]\cdot(3DMF)\}_n$ (1·3DMF)	MnO_4^-	H_2O	0.28 μM	$7.73 \times 10^3\ M^{-1}$	[3]
5.	$\{[Tb(H_2O)(L)(TPA)]\cdot 0.5H_2O\}_n$	MnO_4^-	H_2O	1.43 μM	$1.13 \times 10^4\ M^{-1}$	[4]
6.	$\{[Tb_2(L)_2(H_2O)_2]\cdot 5H_2O\cdot 6DMAC\}_n$	MnO_4^-	H_2O	4.48×10^{-5} mM	$1200\ M^{-1}$	[5]
7.	$[Zn(2,2'bipy)(ppa)(H_2O)_2]\cdot 2H_2O$	MnO_4^-	H_2O	6.73 μM	$3.1 \times 10^4\ M^{-1}$	[6]
8.	$[Tb_4(L)_6(H_2O)_8]$	MnO_4^-	H_2O	0.17 μM	$5.18 \times 10^4\ M^{-1}$	[7]
9.	$[Cd(2\text{-}bpeb)_{0.5}(CNA)(H_2O)]$	MnO_4^-	H_2O	7.79×10^{-5}M	$3.55 \times 10^4\ M^{-1}$	[8]
10.	$[Cd(2\text{-}bpeb)_{0.5}(NDC)]$	MnO_4^-	H_2O	1.31×10^{-4}M	$2.16 \times 1\ 0^4\ M^{-1}$	[8]
11.	$[Zn(2\text{-}bpeb)(BDC)]$	MnO_4^-	H_2O	2.70×10^{-4}M	$1.04 \times 10^4\ M^{-1}$	[8]
12.	$[Tb_2Ni_3(HCAM)_6(H_2O)_{12}]_n$	MnO_4^-	H_2O	0.29 μM	$5.54 \times 10^3\ M^{-1}$	[9]
13.	$[Y_{0.8}Tb_{0.2}(tp)(ox)_{0.5}(H_2O)_2]\cdot H_2O$	MnO_4^-	H_2O	19.6 nM	$5.2\times 10^4\ M^{-1}$	This work

NM = Not Mentioned

Table S5: Comparison of the luminescence-based sensors for the detection of CrO_4^- and $Cr_2O_7^{2-}$ anions

Sl. No.	Luminescent Sensor	Anions Detected	Medium	LOD	K_{sv}	Reference
1.	$[Zn(L)(H_2L)]_n$	$Cr_2O_7^{2-}$	H_2O	11.4 μM	$1.897 \times 10^3 M^{-1}$	10
2.	$\{[Zn(2,5\text{-tdc})(3\text{-abit})]\cdot H_2O\}_n$	CrO_4^{2-} and $Cr_2O_7^{2-}$	H_2O	NM	$5.08 \times 10^3 M^{-1}$ and $5.43 \times 10^3 M^{-1}$	11
3.	$\{[Zn(IPA)(L_2)]\}_n$	CrO_4^{2-} and $Cr_2O_7^{2-}$	H_2O	4 ppm and 4 ppm	$1.00\times10^3 M^{-1}$ and $1.37 \times10^3 M^{-1}$	12
4.	$\{[Cd(IPA)(L_2)]\}_n$	CrO_4^{2-} and $Cr_2O_7^{2-}$	H_2O	1 ppm and 1 ppm	$1.30\times10^3 M^{-1}$ and $2.91 \times10^3 M^{-1}$	12
5.	Ln^{3+}@MIL-121	$Cr_2O_7^{2-}$	H_2O	0.054 μM	$4.34 \times10^3 M^{-1}$	13
6.	$\{[Zn(btz)]_n\}$	CrO_4^{2-} and $Cr_2O_7^{2-}$	H_2O	10 μM and 2 μM	$3.19\times10^3 M^{-1}$ and $4.23\times10^3 M^{-1}$	14
7.	$\{[Zn_2(ttz)H_2O]_n\}$	CrO_4^{2-} and $Cr_2O_7^{2-}$	H_2O	20 μM and 2 μM	$2.35\times10^3 M^{-1}$ and $2.19 \times10^3 M^{-1}$	14
8.	$[\{Zn_2(TPOM)(NH_2\text{-}BDC)_2\}.4H_2O]_n$	CrO_4^{2-} and $Cr_2O_7^{2-}$	DMF	4.8 μM and 3.9 μM	$4.45\times10^3 M^{-1}$ and $7.59 \times10^3 M^{-1}$	15
9.	$\{[Zn_{2.5}(cpbda)(OH)_2]\cdot solvent_2\}_n$	CrO_4^{2-} and $Cr_2O_7^{2-}$	DMF/ DMA: H_2O	NM	NM	16
10.	$[EuL(CH_3COO)Cl]_n$	CrO_4^{2-} and $Cr_2O_7^{2-}$	H_2O	85.4 μM and 86.3 μM	$2.52 \times 10^4 M^{-1}$ and $1.15 \times10^4 M^{-1}$	17
11.	$[Tb_2(H_3L)(C_2O_4)_3(H_2O)_4]\cdot 2H_2O$	CrO_4^{2-} and $Cr_2O_7^{2-}$	H_2O	3.7 μM and 4.2 μM	$3.63 \times 10^3 M^{-1}$and $7.78 \times10^3 M^{-1}$	18
12.	$[Eu_2(tpbpc)_4\cdot CO_3\cdot 4H_2O]\cdot DMF\cdot solvent$	CrO_4^{2-} and $Cr_2O_7^{2-}$	H_2O	0.33 ppm and 1.07 ppm	$7.85 \times 10^3 M^{-1}$ and $1.04 \times10^4 M^{-1}$	19
13.	$[Y_{0.8}Tb_{0.2}(tp)(ox)_{0.5}(H_2O)_2]\cdot H_2O$	CrO_4^{2-} and $Cr_2O_7^{2-}$	H_2O	40.8 nMand 43.9nM	$5.8\times10^4 M^{-1}$and $4.20\times 10^4 M^{-1}$	This work

NM = Not Mentioned

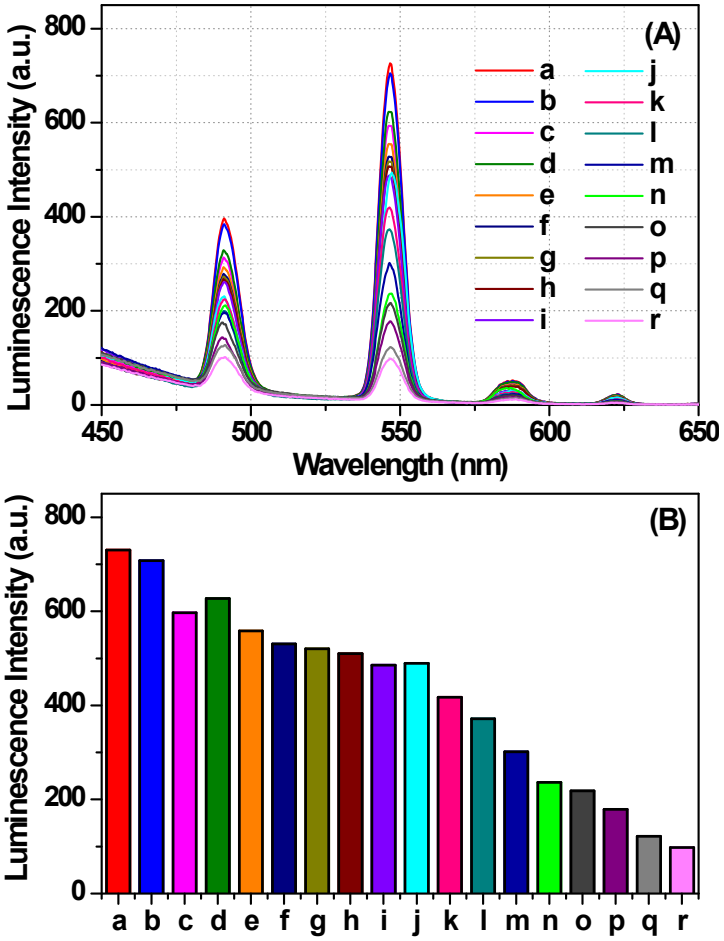

Figure S30. (A) Emission spectra of **1a** in an aqueous solution upon the incremental addition of $HAsO_4^{2-}$ solution in the presence of 12.5 μM of different anion solution (λ_{ex} = 280 nm). (B) Corresponding bar diagram showing the luminescence intensity (monitored at 546 nm) after the sequential addition of the analytes. The composition and concentration of the system were as follows: (a) **1a** in aqueous dispersion, (b) a + 12.5 μM F^-, (c) b + 12.5 μM I^-, (d) c + 12.5 μM Br^-, (e) d + 12.5 μM CO_3^{2-}, (f) e + 12.5 μM SO_4^{2-}, (g) f + 12.5 μM NO_2^-, (h) g + 12.5 μM Cl^-, (i) h + 12.5 μM NO_3^-, (j) i + 12.5 μM CH_3COO^-, (k) j + 12.5 μM $HAsO_4^{2-}$, (l) k + 12.5 μM $HAsO_4^{2-}$, (m) l + 12.5 μM $HAsO_4^{2-}$, (n) m + 12.5 μM $HAsO_4^{2-}$, (o) n + 12.5 μM $HAsO_4^{2-}$, (p) o + 12.5 μM $HAsO_4^{2-}$, (q) p + 12.5 μM $HAsO_4^{2-}$ and (r) q + 12.5 μM $HAsO_4^{2-}$.

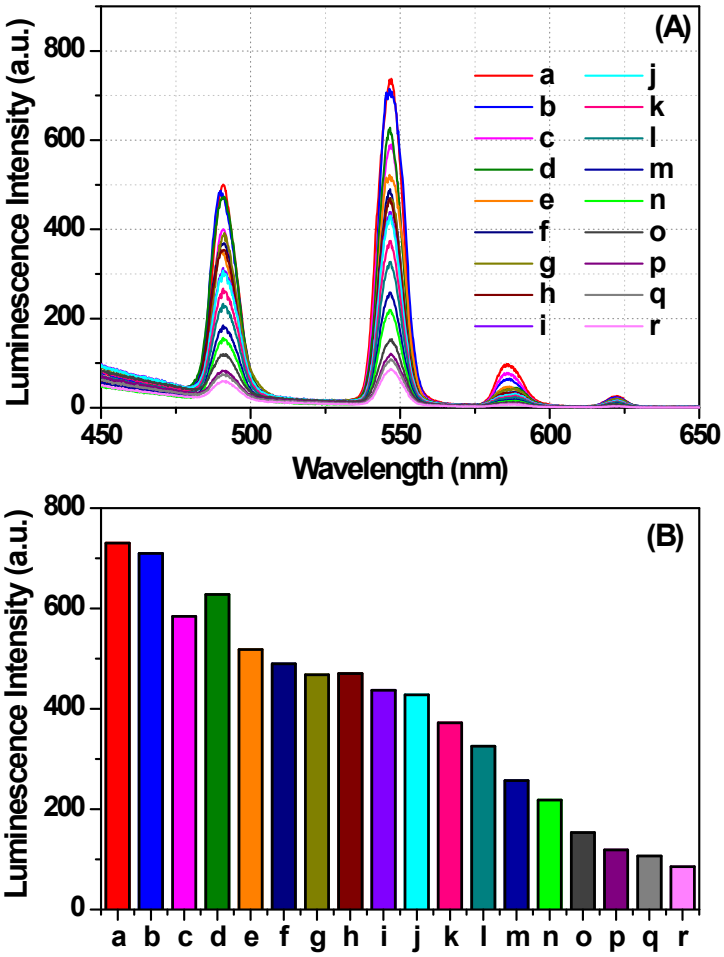

Figure S31. (A) Luminescence spectra of **1a** dispersedin an aqueous solution upon the incremental addition of PO_4^{3-} solution in the presence of 12.5 μM of different anion solution (λ_{ex} = 280 nm). (B) Corresponding bar diagram showing the luminescence intensity (monitored at 546 nm) after the sequential addition of the analytes. The composition and concentration of the system were as follows: (a) **1a** in aqueous dispersion, (b) a + 12.5 μM F^-, (c) b + 12.5 μM I^-, (d) c + 12.5 μM Br^-, (e) d + 12.5 μM CO_3^{2-}, (f) e + 12.5 μM SO_4^{2-}, (g) f + 12.5 μM NO_2^-, (h) g + 12.5 μM Cl^-, (i) h + 12.5 μM NO_3^-, (j) i + 12.5 μM CH_3COO^-, (k) j + 12.5 μM PO_4^{3-}, (l) k + 12.5 μM PO_4^{3-}, (m) l + 12.5 μM PO_4^{3-}, (n) m + 12.5 μM PO_4^{3-}, (o) n + 12.5 μM PO_4^{3-}, (p) o + 12.5 μM PO_4^{3-}, (q) p + 12.5 μM PO_4^{3-} and (r) q + 12.5 μM PO_4^{3-}.

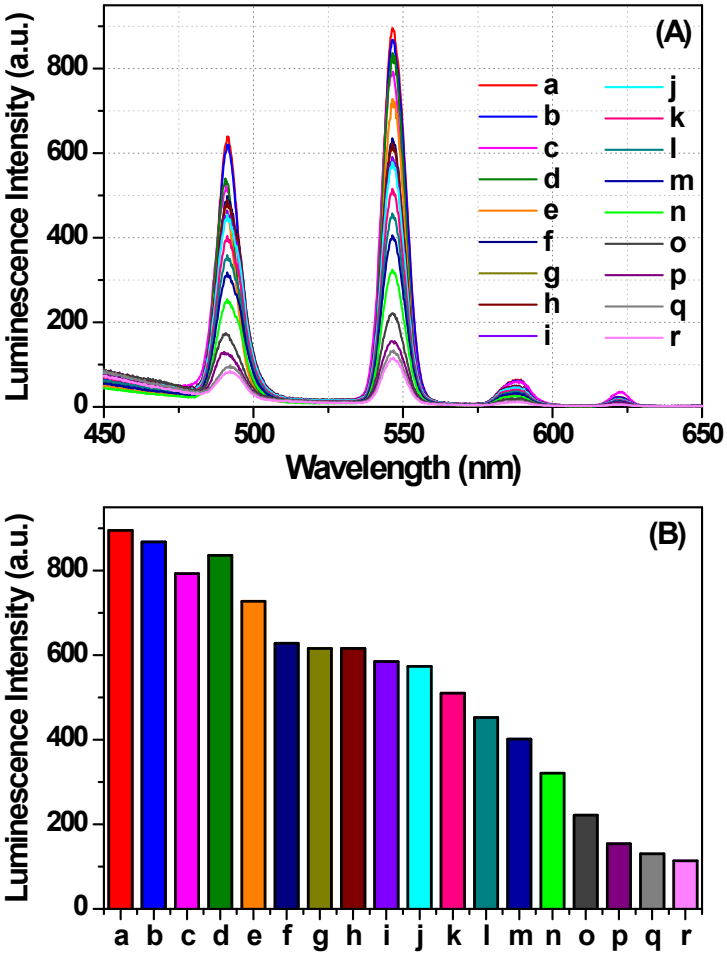

Figure S32. (A) Luminescence spectra of **1a** dispersedin an aqueous solution upon the incremental addition of MnO_4^- solution in the presence of 12.5 μM of different anion solution(λ_{ex} = 280 nm). (B) Corresponding bar diagram showing the luminescence intensity (monitored at 546 nm) after the sequential addition of the analytes. The composition and concentration of the system were as follows: (a) **1a** in aqueous dispersion, (b) a + 12.5 μM F^-, (c) b + 12.5 μM I^-, (d) c + 12.5 μM Br^-, (e) d + 12.5 μM CO_3^{2-}, (f) e + 12.5 μM SO_4^{2-}, (g) f + 12.5 μM NO_2^-, (h) g + 12.5 μM Cl^-, (i) h + 12.5 μM NO_3^-, (j) i + 12.5 μM CH_3COO^-, (k) j + 12.5 μM MnO_4^-, (l) k + 12.5 μM MnO_4^-, (m) l + 12.5 μM MnO_4^-, (n) m + 12.5 μM MnO_4^-, (o) n + 12.5 μM MnO_4^-, (p) o + 12.5 μM MnO_4^-, (q) p + 12.5 μM MnO_4^- and (r) q + 12.5 μM MnO_4^-.

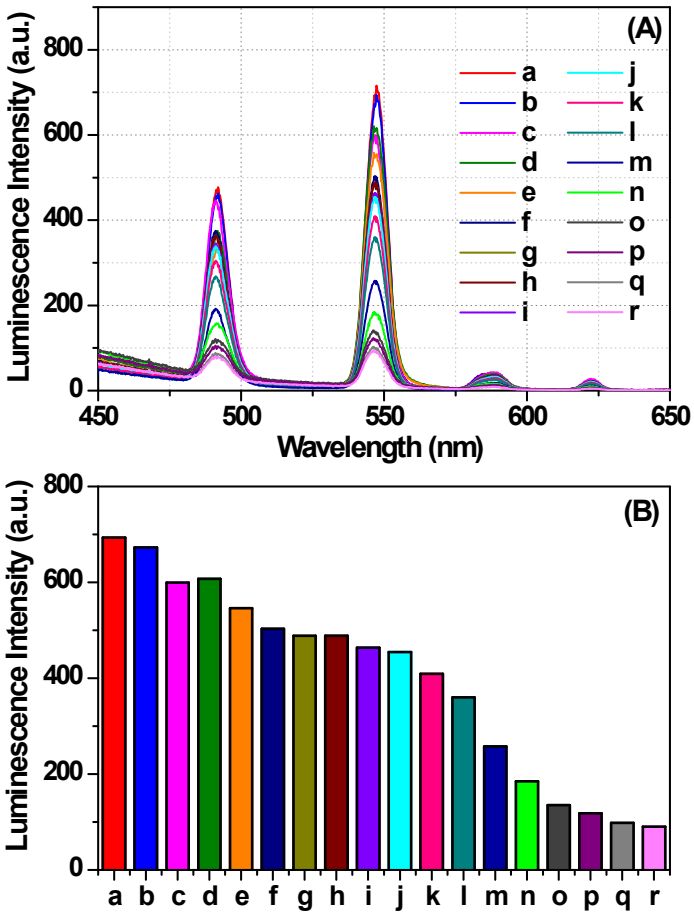

Figure S33: (A) Luminescence spectra of **1a** dispersed in an aqueous solution upon the incremental addition of CrO_4^{2-} solution in the presence of 12.5 μM of different anion solution (λ_{ex} = 280 nm). (B) Corresponding bar diagram showing the luminescence intensity (monitored at 546 nm) after the sequential addition of the analytes. The composition and concentration of the system were as follows: (a) **1a** in aqueous dispersion, (b) a + 12.5 μM F^-, (c) b + 12.5 μM I^-, (d) c + 12.5 μM Br^-, (e) d + 12.5 μM CO_3^{2-}, (f) e + 12.5 μM SO_4^{2-}, (g) f + 12.5 μM NO_2^-, (h) g + 12.5 μM Cl^-, (i) h + 12.5 μM NO_3^-, (j) i + 12.5 μM CH_3COO^-, (k) j + 12.5 μM MnO_4^-, (l) k + 12.5 μM CrO_4^{2-}, (m) l + 12.5 μM CrO_4^{2-}, (n) m + 12.5 μM CrO_4^{2-}, (o) n + 12.5 μM CrO_4^{2-}, (p) o + 12.5 μM CrO_4^{2-}, (q) p + 12.5 μM CrO_4^{2-} and (r) q + 12.5 CrO_4^{2-}.

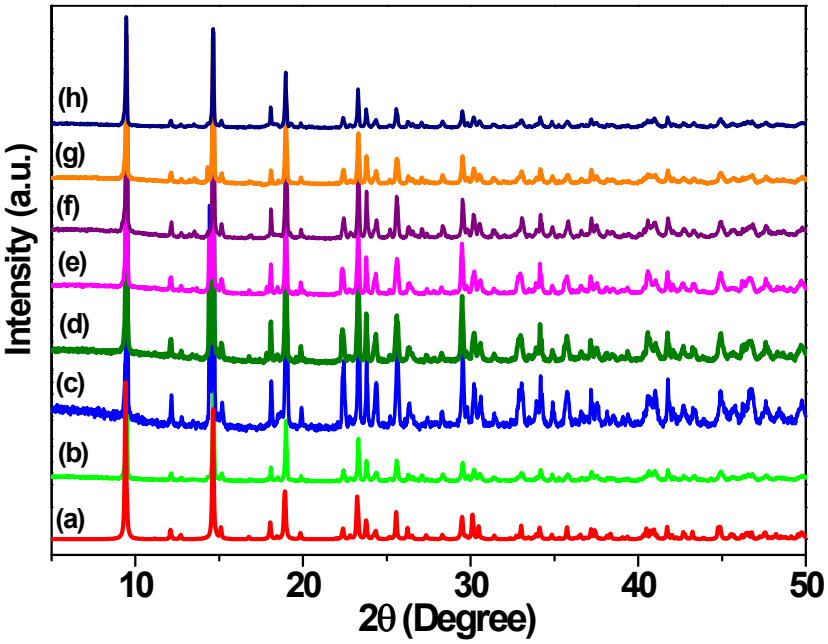

Figure S34. The PXRD pattern of (a) simulated, (b) as-synthesized **1a,** (c) **1a** immersed in water, (d) **1a** immersed in an aqueous solution of $HAsO_4^{2-}$, (e) **1a** immersed in an aqueous solution of PO_4^{3-}, (f) **1a** immersed in an aqueous solution of MnO_4^-, (g) **1a** immersed in an aqueous solution of CrO_4^{2-}, and (h) **1a** immersed in an aqueous solution of $Cr_2O_7^{2-}$.

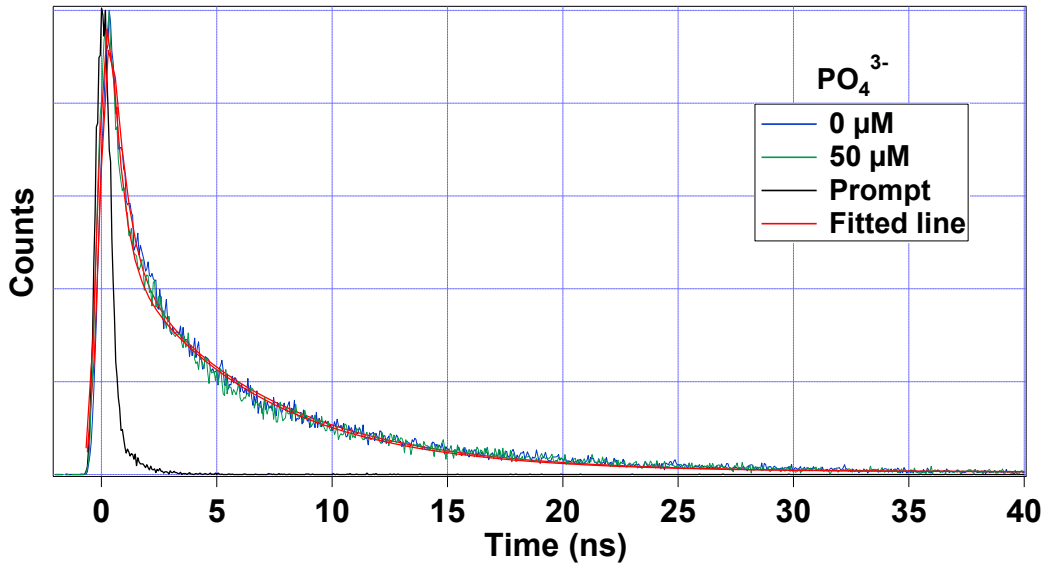

Figure S35. Luminescence lifetime decay profile and the corresponding fitted line of **1a** before and after the addition of PO_4^{3-} anion. The final concentration of PO_4^{3-} ion in the medium is indicated in the legend. The instrument response function (prompt) is also shown. Here, λ_{ex} = 280 nm and λ_{em} = 420 nm (ligand center emission) was set during the experiment.

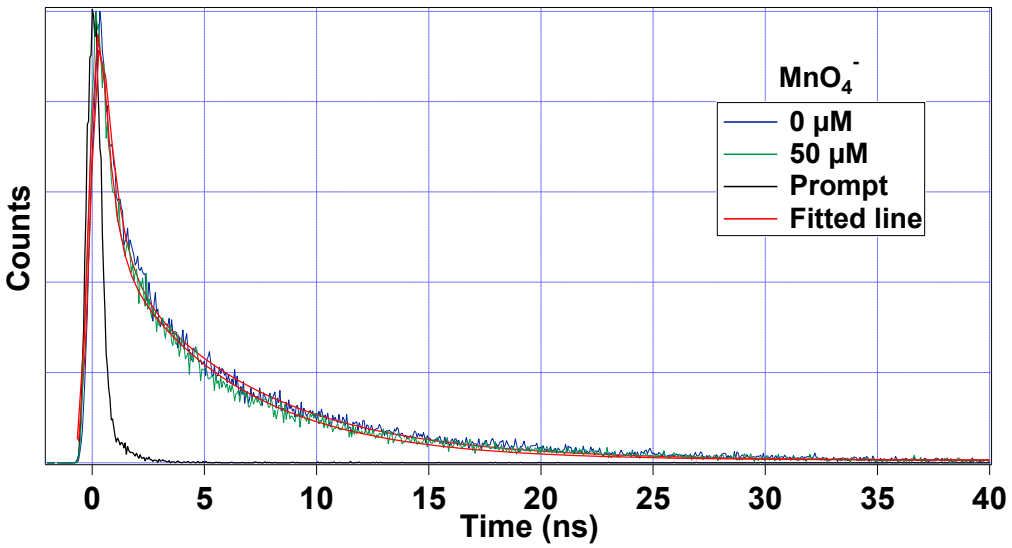

Figure S36. Luminescence lifetime decay profile and the corresponding fitted line of **1a** before and after the addition of MnO_4^- anion. The final concentration of MnO_4^- ion in the medium is indicated in the legend. The instrument response function (prompt) is also shown. Here, λ_{ex} = 280 nm and λ_{em} = 420 nm (ligand center emission) was set during the experiment.

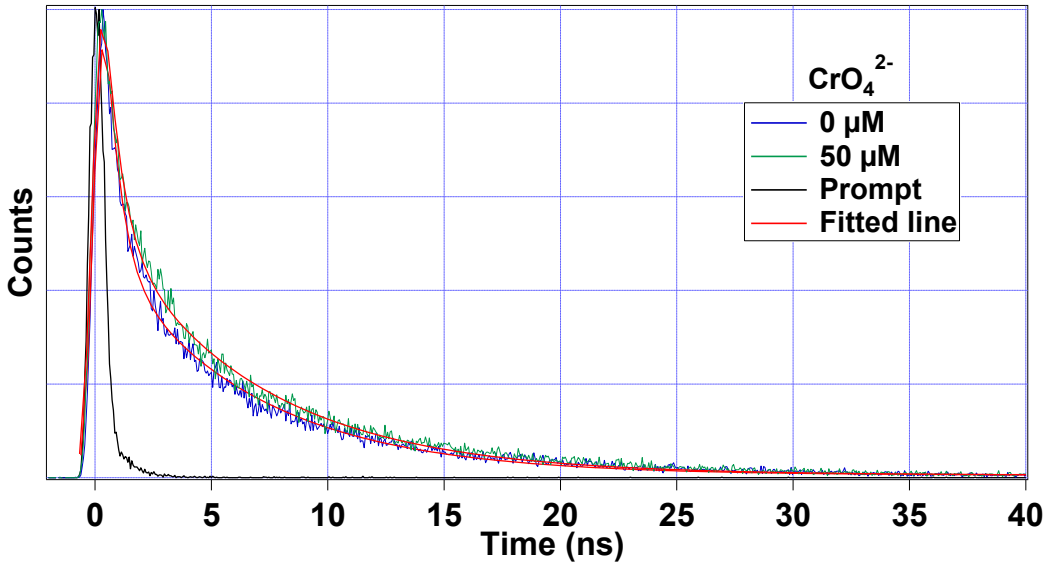

Figure S37. Luminescence lifetime decay profile and the corresponding fitted line of **1a** before and after the addition of CrO_4^{2-}anion. The final concentration of CrO_4^{2-} ion in the medium is indicated in the legend. The instrument response function (prompt) is also shown. Here, λ_{ex} = 280 nm and λ_{em} = 420 nm (ligand center emission) was set during the experiment.

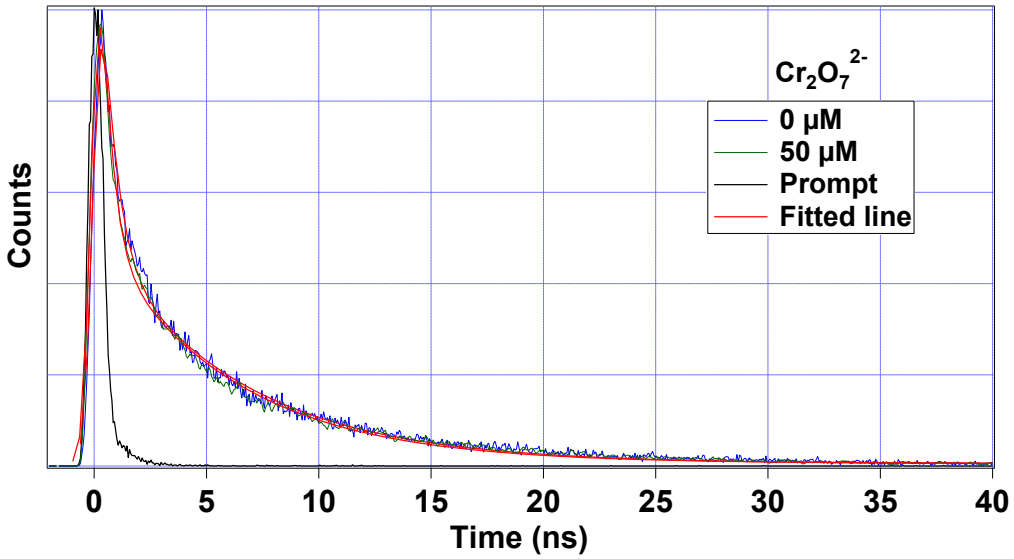

Figure S38. Luminescence lifetime decay profile and the corresponding fitted line of **1a** before and after the addition of $Cr_2O_7^{2-}$ anion. The final concentration of $Cr_2O_7^{2-}$ ion in the medium is indicated in the legend. The instrument response function (prompt) is also shown. Here, λ_{ex} = 280 nm and λ_{em} = 420 nm (ligand center emission) was set during the experiment.

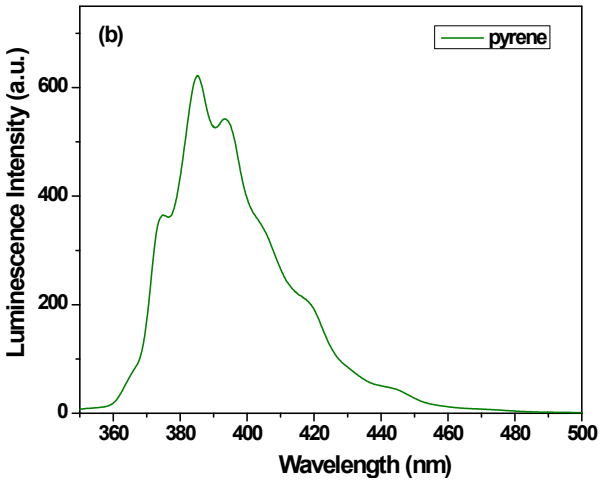

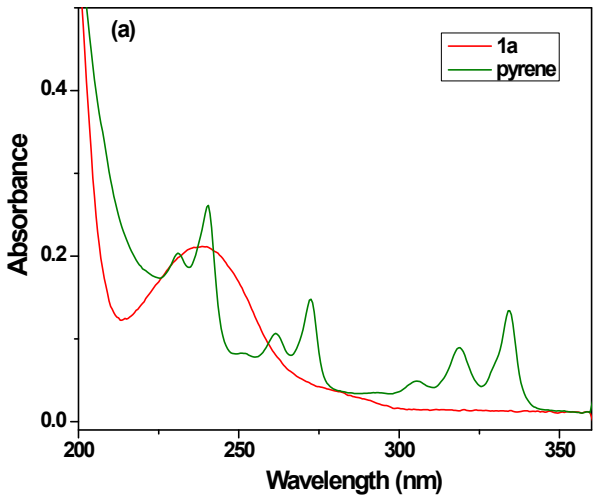

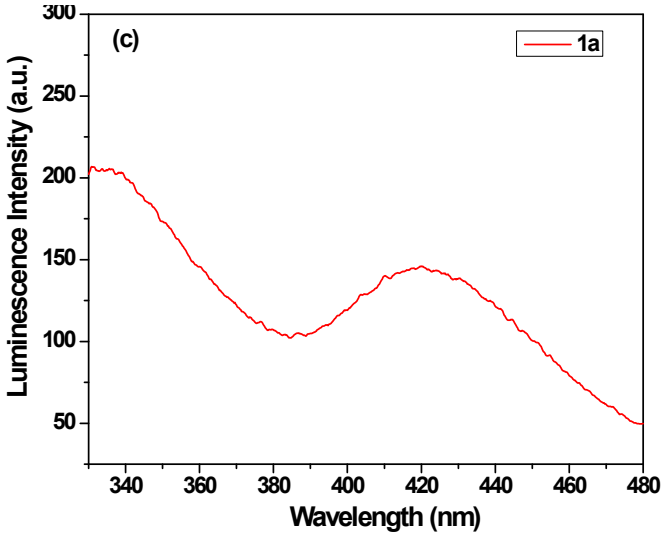

Fig. S39. (a) Absorption spectra of compound **1a** and pyrene, (b) luminescence spectra of pyrene upon excitation at 280 nm and (c) luminescence spectra of compound **1a** upon excitation at 280 nm.

<u>Determination of quantum yield:</u>

$$Q_f^i = \frac{F^i f_s n_i^2}{F^s f_i n_s^2} Q_f^s$$

where Q_f^i and Q_f^s are the fluorescence QYs of the sample and that of the standard, respectively; F^i and F^s are the integrated intensities (areas) of sample and standard spectra, respectively; $f_s and\ f_i$are the absorbance factor of standard and sample, respectively; the refractive indices of the sample and reference solution aren_i and n_s, respectively.

$$Q_f^i = \frac{20944 \times 0.0386 \times 1.33^2}{23084 \times\ 0.037 \times 1.38^2} \times\ 0.3$$

$$Q_f^i =\ 0.26$$

References:

1. A. K. Jana and S. Natarajan, *ChemPlusChem*, 2017, **82**, 1153-1163.
2. Y.-T. Yan, F. Cao, W.-Y. Zhang, S.-S. Zhang, F. Zhang and Y.-Y. Wang, *New J. Chem.*, 2018, **42**, 9865-9875.
3. B. Ding, S. X. Liu, Y. Cheng, C. Guo, X. X. Wu, J. H. Guo, Y. Y. Liu and Y. Li, *Inorg. Chem.*, 2016, **55**, 4391-4402.
4. J.-L. Shi, P. Xu, X.-G. Wang, B. Ding, X.-J. Zhao and E.-C. Yang, *Z. Anorg. Allg. Chem.*, 2018, **644**, 1598-1606.
5. J.-J. Ma and W.-s. Liu, *Dalton Trans.*, 2019, **48**, 12287-12295.
6. K. Wang, M. Zhu, S. Ma, X. Li, M. Zhang and E. Gao, *Polyhedron*, 2019, **166**, 60-64.
7. X. Wang, J.-L. Li, C. Jiang, P. Hu, B. Li, T. Zhang and H.-C. Zhou, *Chem.Commun.*, 2018, **54**, 13271-13274.
8. X.-D. Zhang, Y. Zhao, K. Chen, Y.-F. Jiang and W.-Y. Sun, *Chem. Asian J.*, 2019, **14**, 3620-3626.
9. J. Qian, M.-M. Sun, M. Liu and W. Gu, *ACS Omega*, 2019, **4**, 11949-11959.
10. Y. Wu, Y. Huang, Y. Wang, X. Zou, J. Wang and W. Wu, *J. Coord. Chem.*, 2018, **71**, 3994-4006.
11. J. Zhang, J. Wu, L. Gong, J. Feng and C. Zhang, *ChemistrySelect*, 2017, **2**, 7465-7473.
12. B. Parmar, Y. Rachuri, K. K. Bisht, R. Laiya and E. Suresh, *Inorg. Chem.*, 2017, **56**, 2627-2638.
13. J.-N. Hao and B. Yan, *New J. Chem.*, 2016, **40**, 4654-4661.
14. C.-S. Cao, H.-C. Hu, H. Xu, W.-Z. Qiao and B. Zhao, *Cryst. Eng. Comm.*, 2016, **18**, 4445-4451.
15. R. Lv, J. Wang, Y. Zhang, H. Li, L. Yang, S. Liao, W. Gu and X. Liu, *J. Mater. Chem. A*, 2016, **4**, 15494-15500.
16. W.-H. Huang, J.-Z. Li, T. Liu, L.-S. Gao, M. Jiang, Y.-N. Zhang and Y.-Y. Wang, *RSC Adv.*, 2015, **5**, 97127-97132.
17. C. Chen, X. Zhang, P. Gao and M. Hu, *J. Solid State Chem.*, 2018, **258**, 86-92.
18. C.-Q. Jiao, M. Sun, F. Liu, Y.-N. Zhou, Y.-Y. Zhu, Z.-G. Sun, D.-P. Dong and J. Li, *ACS Omega*, 2018, **3**, 16735-16742.
19. J. Liu, G. Ji, J. Xiao and Z. Liu, *Inorg. Chem.*, 2017, **56**, 4197-4205.